An approximate method for solving rarefied and transitional flows using TDEFM with isotropic mesh adaptation

M.R. Smith*, H.M. Cave†, J.S. Wu† and M.N. Macrossan**

*National Center for High Performance Computing, HsinChu, Taiwan.
†Department of Mechanical Engineering, Jiao Tung University, Hsin-Chu, Taiwan.
**Centre for Hypersonics, The University of Queensland, Brisbane, 4072, Australia

Abstract. DSMC [1] can become increasingly expensive when extended to the near-continuum regime. Because of the statistical nature of the results, long run times are required to build up samples of simulator particles large enough to reduce the statistical scatter to acceptable levels. Here we adapt a kinetic theory based flux method to produce a quick approximate solver for transition and near-continuum flows. The results have no statistical scatter. The CPU times are similar to those of traditional continuum (Navier-Stokes or Euler) solvers. The True Direction Equilibrium Flux Method (TDEFM) [2, 3] is a generalisation of Pullin's kinetic theory based EFM [4]. TDEFM can transfer fluxes of mass, momentum and energy in physically realistic directions from any source cell to any destination cell, even if the cells do not share an interface. TDEFM, as an Euler solver, has been shown to provide good results on a Cartesian grid for flows where standard continuum methods produce unphysical asymmetries apparently because the continuum fluxes are constrained (in one time step) to flow in the grid coordinate directions rather than the correct physical direction. [2, 3] The new method for rarefied flow does not try to produce the correct velocity distribution function, but does ensure that mass, momentum and energy are transported within the flow over the physically correct distances between "pseudo-collisions". To ensure this, (1) the time step is restricted so that mass, momentum and energy are exchanged between contiguous cells only in one time step, and (2) the cells sizes are adapted, as steady state is approached, to be approximately equal to the local mean free path. The results for Mach 5 flow over a flat plate for varying Knudsen numbers show an average difference (compared to DSMC) in the X-velocity profile near the surface of the plate of less than 6 percent. TDEFM, employing adaptive mesh refinement, required less than 9 percent of the computational time required by DSMC for the same flow. Thus the approximate method could be useful for quick "first-estimate" solutions of otherwise time consuming design problems.

Keywords: Kinetic Theory of Gasses, CFD, DSMC, EPSM, EFM, TDEFM, Direct Simulation, Euler Equations, Rarefied Gas Dynamics
PACS: 31.15.Qg, 34.10.+x,47.10.A-,47.11.-j,47.11.Mn,47.45.Ab,47.45.-n

INTRODUCTION

Bird's Direct Simulation Monte-Carlo method [1] simulates a rarefied flow by following the motion and collisions of a large number of simulator particles as they move through the flow. DSMC in the high collision rate limit has been used as an Euler solver [4, 5, 6] and as the 'continuum' part of a hybrid DSMC/continuum solver. DSMC is generally more robust than a conventional Euler solver but suffers from statistical scatter which requires large amounts of CPU power to reduce to acceptable limits. One reason for DSMC's stability is that the fluxes of mass, momentum and energy are carried by particles which move in the physically correct directions; in any time step fluxes may flow from any cell to any other cell in the computational domain.

An important requirement of an accurate direct simulation is that particles are only permitted to move in free flight over realistic distances. Therefore, a accurate DSMC simulation manipulates the time step and cell size such that particles have collisions after moving a distance equivilent to the local mean free path. The cell size Δx dictates the size of the region from which properties are sampled. These properties control the calculated collision rate, and thus affect all particles within that region. Where the characteristic length of these gradients approach λ, the cell size must also. In regions where the flow gradients are small or zero, such a restriction is not required. Alexander [7, 8] shows that the effective viscosity and heat transfer present are functions of the cell size.

Presented is the True Direction Equilibrium Flux Method (TDEFM) employed using an Adaptive Refined Mesh (AMR). TDEFM aims to maintain the analytical foundation of EFM while employing the physical mechanism of transport employed by a direct solver such as DSMC. The fluxes of mass, momentum and energy are determined by integration of the local Maxwell-Boltzmann distribution over both velocity space and the physical volume of

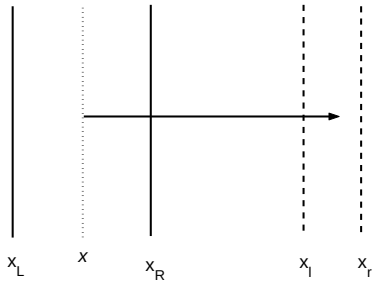

FIGURE 1. Particle moving from x (between x_L and x_R) to a region between x_l and x_r. For the derivations used here, $x_r \geq x_l$ & $x_R \geq x_L$

each cell. This novel approach allows fluxes to be transported from any specified source volume to any specified destination volume. Unlike EFM, flux exchange between cells is not limited to those sharing adjacent interfaces. The fluxes obtained using TDEFM represent the analytical solution to the free flight phase of a direct simulation in the limit of an infinite number of simulation particles for any time step when conditions in each cell are uniform and in thermal equilibrium. By employing AMR to ensure the cell size is approximately equal to the local mean free path, the numerical dissipation inherent in TDEFM is approximately equal to the physically realistic dissipation. While no effort is made to correctly capture the non-equilibrium distributions present in rarefied and transitional flows, moving the molecules in free flight over physically realistic distances and directions is shown to provide results approximately equal to those obtained using full DSMC for a fraction of the computational expense.

TDEFM

Derived below are the expressions for the mass, momentum and energy carried by molecules in free-molecular flight for time Δt, starting from a rectangular region (in 2D) to any other rectangular region. For simplicity all forces acting on particles are assumed to be zero, *i.e.* no particle interactions occur while particles are moving. Internal structural energy (such as energy due to rotation and vibration) is included in the energy flux expressions so monatomic, diatomic or polyatomic gases can be simulated.

Uniform conditions are assumed within the cell from which the molecules originate (*i.e.* there are no gradients of density, mean velocity or temperature within the cell) and all the molecules within the cell have velocities conforming to the same Maxwell-Boltzmann distribution. The distribution function in one dimension has the Maxwell-Boltzmann form

$$g(v) = \frac{1}{\sqrt{2\pi}s} \exp\left(\frac{-(v-m)^2}{2s^2}\right) \tag{1}$$

where

$$m = \int_{-\infty}^{\infty} v g(v)\, dv \text{ and } s = (RT)^{-1/2}.$$

In other words, the fraction of molecules having a velocity v_x in the range $v_x \rightarrow v_x + dv_x$ is $g(v_x)\, dv_x$ and similar expressions hold for v_y and v_z. The velocity required by a particle at location x to travel in free molecular flight and fall into the region bounded by x_l and x_r (shown in Figure 1) is between $\frac{x_l - x}{t}$ and $\frac{x_r - x}{t}$. Therefore, the chance of a particle at position x moving to between $x_l - x_r$ is:

$$\begin{aligned} p(x) &= \int_{\left(\frac{x_l - x}{\Delta t}\right)}^{\left(\frac{x_r - x}{\Delta t}\right)} \frac{1}{\sqrt{2\pi}s} \exp\left(\frac{-(v_x - m)^2}{2s^2}\right) dv_x \\ &= \frac{1}{2}\left[\text{erf}\left(\frac{m\Delta t + x - x_l}{\sqrt{2}s\Delta t}\right) - \text{erf}\left(\frac{m\Delta t + x - x_r}{\sqrt{2}s\Delta t}\right)\right] \end{aligned} \tag{2}$$

The average probability of a particle having the required velocity range over the space $x_L - x_R$ represents the fraction of particles from the region between x_L and x_R possessing the velocities specified and is given by:

$$\begin{aligned} f_M &= \frac{1}{(x_R - x_L)} \int_{x_L}^{x_R} p(x)dx \\ &= \mathbf{f}_{\mathrm{M}}(\mathrm{m}, \mathrm{s}, \Delta\mathrm{t}, \mathrm{x_R}, \mathrm{x_L}, \mathrm{x_l}, \mathrm{x_r}) \qquad (3) \\ &= M_c \exp\left(\frac{-(m\Delta t + x_R - x_l)^2}{2s^2\Delta t^2}\right) + M_1 \mathrm{erf}\left(\frac{m\Delta t + x_R - x_l}{\sqrt{2}s\Delta t}\right) \\ &- M_c \exp\left(\frac{-(m\Delta t + x_R - x_r)^2}{2s^2\Delta t^2}\right) - M_2 \mathrm{erf}\left(\frac{m\Delta t + x_R - x_r}{\sqrt{2}s\Delta t}\right) \\ &- M_c \exp\left(\frac{-(m\Delta t + x_L - x_l)^2}{2s^2\Delta t^2}\right) - M_3 \mathrm{erf}\left(\frac{m\Delta t + x_L - x_l}{\sqrt{2}s\Delta t}\right) \\ &+ M_c \exp\left(\frac{-(m\Delta t + x_L - x_r)^2}{2s^2\Delta t^2}\right) + M_4 \mathrm{erf}\left(\frac{m\Delta t + x_L - x_r}{\sqrt{2}s\Delta t}\right) \end{aligned}$$

(4)

This equation can be used to find the fraction of mass from region $x_L \leftrightarrow x_R$ that flows into the region between $x_l \leftrightarrow x_r$. The constants M_c and $M_1 - M_4$ are easily determined [2]. The momentum and energy transfer (per unit source mass) is found by taking moments of the equilibrium distribution function and are [2]:

$$\begin{aligned} f_P &= \mathbf{f}_{\mathrm{P}}(\mathrm{m}, \mathrm{s}, \Delta\mathrm{t}, \mathrm{x_R}, \mathrm{x_L}, \mathrm{x_l}, \mathrm{x_r}) \qquad (5) \\ &= P_c \exp\left(\frac{-(m\Delta t + x_R - x_l)^2}{2s^2\Delta t^2}\right) + P_1 \mathrm{erf}\left(\frac{m\Delta t + x_R - x_l}{\sqrt{2}s\Delta t}\right) \\ &- P_c \exp\left(\frac{-(m\Delta t + x_R - x_r)^2}{2s^2\Delta t^2}\right) - P_2 \mathrm{erf}\left(\frac{m\Delta t + x_R - x_r}{\sqrt{2}s\Delta t}\right) \\ &- P_c \exp\left(\frac{-(m\Delta t + x_L - x_l)^2}{2s^2\Delta t^2}\right) - P_3 \mathrm{erf}\left(\frac{m\Delta t + x_L - x_l}{\sqrt{2}s\Delta t}\right) \\ &+ P_c \exp\left(\frac{-(m\Delta t + x_L - x_r)^2}{2s^2\Delta t^2}\right) + P_4 \mathrm{erf}\left(\frac{m\Delta t + x_L - x_r}{\sqrt{2}s\Delta t}\right) \end{aligned}$$

(6)

$$\begin{aligned} f_E &= \mathbf{f}_{\mathrm{E}}(\mathrm{m}, \mathrm{s}, \Delta\mathrm{t}, \mathrm{x_R}, \mathrm{x_L}, \mathrm{x_l}, \mathrm{x_r}) \qquad (7) \\ &= E_c \exp\left(\frac{-(m\Delta t + x_R - x_l)^2}{2s^2\Delta t^2}\right) + E_1 \mathrm{erf}\left(\frac{m\Delta t + x_R - x_l}{\sqrt{2}s\Delta t}\right) \\ &- E_c \exp\left(\frac{-(m\Delta t + x_R - x_r)^2}{2s^2\Delta t^2}\right) - E_2 \mathrm{erf}\left(\frac{m\Delta t + x_R - x_r}{\sqrt{2}s\Delta t}\right) \\ &- E_c \exp\left(\frac{-(m\Delta t + x_L - x_l)^2}{2s^2\Delta t^2}\right) - E_3 \mathrm{erf}\left(\frac{m\Delta t + x_L - x_l}{\sqrt{2}s\Delta t}\right) \\ &+ E_c \exp\left(\frac{-(m\Delta t + x_L - x_r)^2}{2s^2\Delta t^2}\right) + E_4 \mathrm{erf}\left(\frac{m\Delta t + x_L - x_r}{\sqrt{2}s\Delta t}\right) \end{aligned}$$

where C is a molecules internal structural energy and includes any energy held in unused translational degrees of freedom. The value of C, together with the constants $P_c, P_1 - P4, E_c$ and $E_1 - E_4$ can be found in [2].

2D ADAPTIVE MESH REFINEMENT

Due to the employment of adaptive mesh refinement knowledge of neighbouring cell size and location cannot be incorporated easily into the flux expressions themselves. While a set of situation specific flux expressions could be

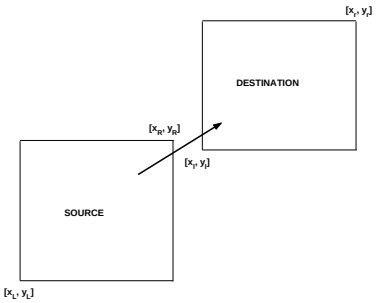

FIGURE 2. Sample source and destination cell geometry in 2D. The source cell is bounded by the coordinates $(x_L, y_L) - (x_R, y_R)$. The destination cell is bounded by the coordinates $(x_l, y_l) - (x_r, y_r)$.

created and employed for different possible source cell - destination cell combinations, it is far easier (although computationally expensive) to simply calculate the full TDEFM flux. Referring to Figure 2, the net flux of mass, momentum and energy to move from the source region to the destination region is:

$$\begin{aligned}
M &= M_0 \mathbf{f}_{\mathrm{M}}(\mathrm{U}, \sqrt{\mathrm{RT}}, \Delta\mathrm{t}, \mathrm{x_R}, \mathrm{x_L}, \mathrm{x_l}, \mathrm{x_r}) \times \mathbf{f}_{\mathrm{M}}(\mathrm{V}, \sqrt{\mathrm{RT}}, \Delta\mathrm{t}, \mathrm{y_R}, \mathrm{y_L}, \mathrm{y_l}, \mathrm{y_r}) \\
P_x &= M_0 \mathbf{f}_{\mathrm{P}}(\mathrm{U}, \sqrt{\mathrm{RT}}, \Delta\mathrm{t}, \mathrm{x_R}, \mathrm{x_L}, \mathrm{x_l}, \mathrm{x_r}) \times \mathbf{f}_{\mathrm{M}}(\mathrm{V}, \sqrt{\mathrm{RT}}, \Delta\mathrm{t}, \mathrm{y_R}, \mathrm{y_L}, \mathrm{y_l}, \mathrm{y_r}) \\
P_y &= M_0 \mathbf{f}_{\mathrm{M}}(\mathrm{U}, \sqrt{\mathrm{RT}}, \Delta\mathrm{t}, \mathrm{x_R}, \mathrm{x_L}, \mathrm{x_l}, \mathrm{x_r}) \times \mathbf{f}_{\mathrm{P}}(\mathrm{V}, \sqrt{\mathrm{RT}}, \Delta\mathrm{t}, \mathrm{y_R}, \mathrm{y_L}, \mathrm{y_l}, \mathrm{y_r}) \\
E_x &= M_0 \mathbf{f}_{\mathrm{E}}(\mathrm{U}, \sqrt{\mathrm{RT}}, \Delta\mathrm{t}, \mathrm{x_R}, \mathrm{x_L}, \mathrm{x_l}, \mathrm{x_r}) \times \mathbf{f}_{\mathrm{M}}(\mathrm{V}, \sqrt{\mathrm{RT}}, \Delta\mathrm{t}, \mathrm{y_R}, \mathrm{y_L}, \mathrm{y_l}, \mathrm{y_r}) \\
E_y &= M_0 \mathbf{f}_{\mathrm{M}}(\mathrm{U}, \sqrt{\mathrm{RT}}, \Delta\mathrm{t}, \mathrm{x_R}, \mathrm{x_L}, \mathrm{x_l}, \mathrm{x_r}) \times \mathbf{f}_{\mathrm{E}}(\mathrm{V}, \sqrt{\mathrm{RT}}, \Delta\mathrm{t}, \mathrm{y_R}, \mathrm{y_L}, \mathrm{y_l}, \mathrm{y_r}) \\
E &= E_x + E_y
\end{aligned}$$

where M, P and E are the net mass, momentum and energy fluxes respectively, M_0 is the initial mass in the source region, and $([x_L, y_L], [x_R, y_R])$ give the size and location of the rectangular source region, $([x_l, y_l], [x_r, y_r])$ describe the size and location of the destination region, U is the X velocity, V is the Y velocity, M is the net mass flux, P_x and P_y are the X and Y momentum fluxes and E is the energy flux. These fluxes of mass, momentum and energy represent the analytical fluxes where molecules belonging to a gas in thermal equilibrium are moved in free molecular flight. The destination region can be located anywhere in space and is not required to be adjacent to the source region.

The proposed implementation is applied to the calculation of steady flows and is seperated into 3 phases. First, the steady flow is calculated on a relatively coarse mesh. Where cells are larger than the 1.5 times the local mean free path, they are flagged for division. Each cell can only be divided once per time step. The solution is advanced in time to allow the flow to adjust to the new computational grid between mesh adaptations. Finally, any cells which are smaller than half the local mean free path are flagged for combination. Likewise, a set of cells can only be combined once per timestep. The cell division routine for a cell k is outlined below:

1. Create 3 new cells with indexes of $N+1, N+2$ and $N+3$, where N was the previous number of existing cells (including ghost cells).
2. Evenly distribute the mass, momentum and energy amoung cells k, $N+1, N+2$ and $N+3$.
3. Calculate the state in the newly created cells and regenerate the local neighbour list. A complete reconstruction of the neighbour list is not required - just a reconstruction of the cells which were previously neighbours of cell k.
4. Search through all neighbours of cell k. If the neighbour is a ghost cell and adjacent to cell k, it should also be split.
5. Update the total number of cells.

By employing strict rules for the creation of new cells, the process of cell combination is simplified. When cells are flagged for combination, the mass, momentum and energy is summed and assigned to the memory allocated for cell k. The previous cells are deleted and the entire list of cells (and their neighbours) are adjusted.

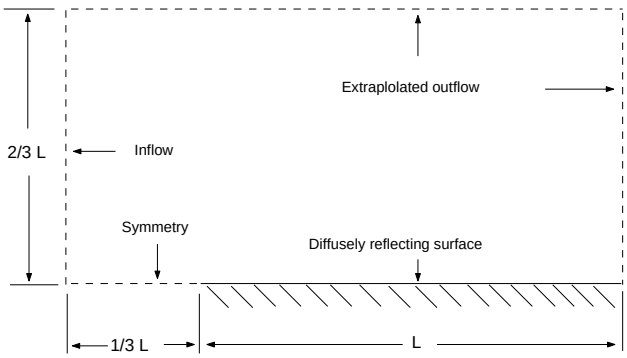

FIGURE 3. Computational domain used for simulation of hypersonic flow over a flat plate. The physical geometry is fixed in both TDEFM and DSMC computations. The knudsen number is varied through manipulation of the gas viscosity alone.

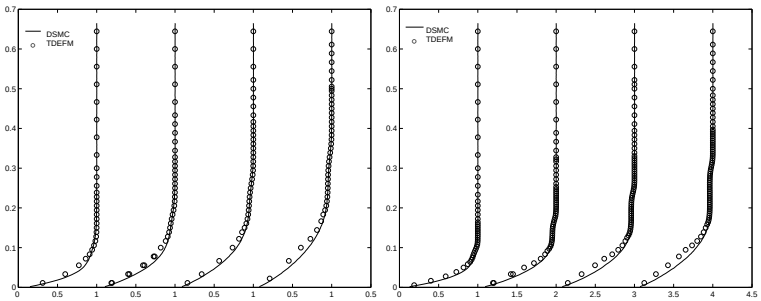

FIGURE 4. X-velocity profiles from TDEFM for simulation of hypersonic flow over a flat plate. Each line represents the variation in x-velocity at $x/L = 0.2, 0.4, 0.6$ and 0.8. The Knudsen numbers for each case are $Kn = 0.01$ (Left) and $Kn = 0.005$ (Right). The gas is monatomic with a power law based viscosity. Adaptive Mesh Refinement (AMR) is employed to ensure the cell size is approximately equal to the local mean free path.

RESULTS

Results from a hypersonic flow over a flat plate are shown. The employed computational domain is shown in Figure 3. The simulated gas is an ideal, monatomic hypothetical gas with a power law viscosity ($\omega = 0.81$). The mach number of the freestream gas is $M_\infty = 5$. The temperature of the plate is fixed at the freestream temperature. The top and right hand side boundaries are extrapolated outflow. The left hand side boundary is inflow while the lower surface located infront of the diffusely reflective surface is specularly reflective. The Knudsen number of the flow is varied to test the general capability of the adaptive grid TDEFM technique. This is done through manipulation of the gas viscosity - the physical geometry is fixed in its dimensions.

The results from TDEFM are compared to results taken from a DSMC solution. The number of simulation particles employed varied with the simulated Knuden number. Due to it's proven performance, Wu's parallel DSMC solver PDSC [9] with a variable hard sphere molecular model was used. Each simulation was run parallel over a 12 processor cluster. Each DSMC solution employed adaptive time stepping on a regular cartesian grid with adaptive sub-cells. The diffusely reflecting surface is completely accomodating.

To compare the results obtained by DSMC and TDEFM, x-velocity and density profiles at regular locations along the plate are examined. Figure 4 shows the x-velocity as a function of distance from the plate surface at locations $x/L = 0.06, 0.33, 0.66$ and 0.86 for varying Knudsen numbers. The gradient of velocity at the plate surface calculated by TDEFM closely matchese that obtained by the DSMC results. There is generally very good agreement between the TDEFM and DSMC results over the entire flow field.

Figure 5 shows the density as a function of distance from the plate surface at locations $x/L = 0.06, 0.33, 0.66$ and 0.86 for varying Knudsen numbers. The differences between the TDEFM and DSMC results are more obvious - the thickness of the shock is larger in the TDEFM results than in the DSMC results. This is likely because of DSMC's ability to maintain information regarding mass distribution across cells. TDEFM forces uniform mass distribution

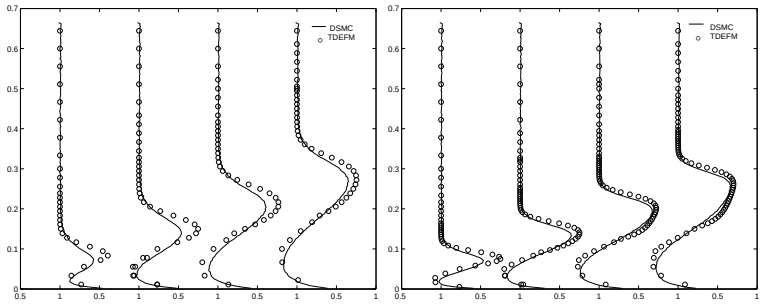

FIGURE 5. Density profiles from TDEFM for simulation of hypersonic flow over a flat plate. Each line represents the variation in density at $x/L = 0.2, 0.4, 0.6$ and 0.8. The Knudsen numbers for each case are $Kn = 0.01$ (Left) and $Kn = 0.005$ (Right). The gas is monatomic with a power law based viscosity. Adaptive Mesh Refinement (AMR) is employed to ensure the cell size is approximately equal to the local mean free path.

across each cell at each time step. Despite the large numbers of cells, the computational expense of using TDEFM with adaptive mesh refinement is still significantly less than using conventional DSMC, requiring less than 4 percent of the computation time required by PDSMC.

CONCLUSION

The True Direction Equilibrium Flux Method (TDEFM) is presented here with the aim of reproducing the results obtained by the direct simulation technique DSMC. In TDEFM the integrals of the equilibrium distribution function are evaluated over both velocity space and the entire physical space of the cell, rather than just at the boundary. The fluxes of mass, momentum and energy are carried from any specified source region into any specified destination region. These fluxes are not limited to cells sharing adjacent interfaces and can, for a given time step, be exchanged between any source and destination cell. TDEFM is the analytical equivalent to EPSM when conditions in each cell are uniform and an infinite number of simulation particles are present. By utilising an adaptive mesh where the desired cell size is based on a fraction of the local mean free path length and newly derived diffusely reflective flux expressions, the TDEFM fluxes are shown to approximately reproduce results obtained by DSMC for a viscous flow.

REFERENCES

1. Bird, G.A., *Molecular Gas Dynamics and the direct simulation of gas flows*, Clarendon Press, Oxford, 1994.
2. Smith, M.R., Macrossan, M.N. and Abdel-Jawad, M.M, 'Effects of Direction Decoupling in flux calculation in Euler Solvers', *Journal of Computational Physics*, **227**:4142-4161, 2008.
3. Macrossan, M.N., Smith, M.R., Metchnik, M. and Pinto, P.A.,'True Direction Equilibrium Flux Method: Applications on Rectangular 2D Meshes', In *Proceedings of the 25th International Symposium on Rarefied Gas Dynamics*, Edited by M.S. Ivanov and A. K. Rebrov, Siberian Branch of the Russian Academey of Sciences : 239-244, 2007. : 239-244, 2007.
4. Pullin, D.I., 'Direct Simulation Methods for Compressible Ideal Gas Flow',*J. Comput. Phys.* **34**: 231-244, 1980.
5. Merkle, C.L., Behrens, H.W. and Hughes, R.D., 'Application of the Monte-Carlo Simulation Procedure in the Near Continuum Regime', *in Rarefied Gas Dynamics*, edited by S. S. Fisher, Prog. Astro. Aero. v74, AIAA, New York, 1981.
6. Lengrand, J.C., Raffin, M. and Allegre, J., *Monte Carlo Simulation Method Applied to Jet Wall Interactions under Continuum Flow Conditions*, in Rarefied Gas Dynamics, edited by S.S Fisher, Prog. Astro. Aero. V.74, AIAA, New York, 994-1006, 1981.od Applied to Jet Wall Interactions under Continuum Flow Conditions, in Rarefied Gas Dynamics, editied by S.S Fisher, Prog. Astro. Aero. V.74, AIAA, New York, 994-1006, 1981.
7. Alexander, F.J., Garcia, A.L. and Alder, B.J., 'Cell size dependence of transport coefficients in stochastic particle algorithms', *Physics of Fluids*, **10(6)** : 1540 - 1542, 1998.
8. Alexander, F.J., Garcia, A.L. and Alder, B.J., 'Erratum: 'Cell size dependence of transport coefficients in stochastic particle algorithms', *Physics of Fluids* 10, 1540 (1998)', *Physics of Fluids*, **12(3)** : 731, 2000.
9. Wu,J.-S., Tseng, K.-C and Wu, F.-Y., 'Parallel three dimensional DSMC method using mesh refinement and variable time-step scheme', *Computer Physics Communications*, **162(3)**:166-187, 2004.